

# Review Paper

## Melt-Texturing Processes of HTS\*

Kamel Salama & Dominic F. Lee†

Mechanical Engineering Department and Texas Center for Superconductivity, University of Houston, Houston, TX 77204-4792, USA

(Received 4 June 1995; accepted 25 July 1995)

**Abstract:** The most promising method to achieve large current capacity in bulk  $\text{YBa}_2\text{Cu}_3\text{O}_x$  is melt-texturing, which so far has provided the highest  $J_c$  reported for bulk HTS at 77 K. In this process, a microstructure with a high degree of grain orientation is developed. By systematic development of optimum processing conditions,  $J_c$  ranging from  $10^5$  A/cm<sup>2</sup> at self-field to  $10^4$  A/cm<sup>2</sup> at a few Tesla, has been achieved. With the development of directional solidification methods and seeding, the problem of domain size restriction promises to be surmountable. Moreover, it may be possible to circumvent the slow solidification rate of textured HTS through recrystallization methods.

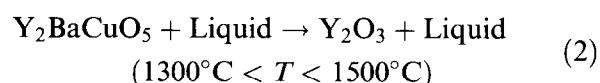
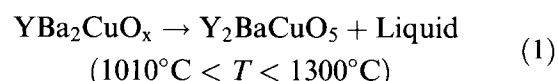
### 1 INTRODUCTION

With the discovery of high-temperature superconductivity in 1986, technologies that were previously prohibitive because of the high cost of cryogen seemed to be readily feasible. However, bulk-sintered high-temperature superconductors (HTS) were found to possess extremely low transport-critical current densities ( $J_c$ ),<sup>1</sup> and HTS seemed destined to be regarded as mere scientific curiosity. However, the feverish pace of HTS research was again rekindled in 1989 when it was shown that melt-texturing of the  $\text{YBa}_2\text{Cu}_3\text{O}_x$  (123) superconductor can result in large  $J_c$ .<sup>2</sup> Since then, there has been significant progress in improving both the self-field  $J_c$  and its behaviour in an applied field. In this paper, various melt-processing

methods will be reviewed, and their  $J_c$  characteristics presented.

### 2 MELT-TEXTURING OF $\text{YBa}_2\text{Cu}_3\text{O}_x$

Melt-texturing of bulk 123 results in a superconductor consisted of thin plates stacked along the  $c$ -axis. When a current flows along the extensive  $a$ - $b$  planes, it encounters no grain boundary, thereby resulting in a self-field  $J_c$  of the order of  $10^5$  A/cm<sup>2</sup>.<sup>3</sup> All melt-texturing methods involve the melting of 123 above its peritectic temperature according to the following reactions:



On subsequent heat treatment, 123 forms during solidification or recrystallization, resulting in the familiar textured microstructure. Since the initial effort in melt-texturing, a number of melt-processing methods have been developed. These methods can be classified into five main categories: (i) slow solidification from the melt in the absence of a temperature gradient, (ii) slow solidification from the melt in a temperature gradient without sample transport, (iii) slow solidification from the melt in a temperature gradient with sample transport, (iv) slow solidification through seeding, and (v) rapid recrystallization in a temperature gradient. In addition to these primary methods, modifications by varying the starting stoichiometry, the precursor compounds and the addition of secondary phases have also been studied.<sup>4–6</sup>

#### 2.1 Nondirectional melt-texturing

Melt-texturing methods belonging to the first two categories are nondirectional processes. On slow cooling, 123 nuclei form in the semi-solid melt and grow independently resulting in a bulk

\*This work is supported by ARPA and the State of Texas.

†New address: M&C Division, Oak Ridge National Laboratory, TN 37831, USA.

superconductor consisting of multiple oriented domains that are misaligned with respect to each other. Melt-texturing was first developed by Jin *et al.*<sup>2</sup>, who termed their process melt textured growth (MTG). In this method, presintered 123 bars are melted at 1050–1200°C, followed by cooling to 900°C at a rate of roughly 12°C/h in the presence of a 50°C/cm temperature gradient. Since the cooling rate is relatively high, the resulting 123 grains are found to be needle-shaped and nearly parallel to each other. Realizing the importance of slow cooling, Salama *et al.*<sup>7</sup> developed a liquid phase processing (LPP) method, which provides the now-familiar stacked plate microstructure. In the LPP method, presintered 123 bars are introduced vertically into a furnace preheated to 1100°C. After approximately 15–20 min, the samples are rapidly cooled to a temperature slightly above the 123 peritectic temperature, and slow cooling is commenced at a rate of 0.5–2°C/h to 925°C. During slow cooling, nucleation and growth of the 123 superconductor occur, and the stacked plate microstructure is developed. Because of incomplete peritectic recombination, 10–15 vol% oblong  $\text{Y}_2\text{BaCuO}_5$  (211) precipitates, 2–20  $\mu\text{m}$  in size, are typically found in the microstructure.

Several investigators<sup>8,9</sup> have proposed that the growth of 123 does not occur through the typical peritectic reaction and transformation processes. Instead, the growth of 123 is believed to be Y-diffusion controlled, where Y is provided by the dissolution of 211 particles ahead of the growth front. Consequently, the maximum stable growth rate is limited by the diffusion distance and, therefore, the average 211 particle size. However, the relatively large 211 precipitates in the LPP 123 microstructure indicate that significant 211 coarsening occurs in the 211 + liquid semi-solid state.<sup>10</sup> In order to reduce the 211 particle size and increase the growth rate, Murakami *et al.*<sup>11</sup> developed a melt powder melt growth process (MPMG), which takes advantage of the second peritectic reaction that occurs at a higher temperature (eqn (2)). In this process, 123 is heated in a Pt boat to 1450°C, where it decomposes into  $\text{Y}_2\text{O}_3$  solid and a liquid phase, and the semi-solid is then rapidly quenched to room temperature. After grinding and pressing, the quenched material containing homogeneously distributed fine  $\text{Y}_2\text{O}_3$  particles is reheated to 1100°C and held at this temperature for 30–60 min. During this holding period,  $\text{Y}_2\text{O}_3$  particles react with the liquid to form fine 211 particles. After the phase conversion, the sample is rapidly cooled to 1000°C and then slow cooled at a rate of 1–5°C/h to 950°C. Because of the smaller initial 211 particle

size, the 211 particles found within the MPMG microstructure are typically 2  $\mu\text{m}$  and less.

In addition to these basic methods, numerous modifications have resulted in subtle microstructure differences. These include the use of Y-rich starting material,<sup>4</sup> 211<sup>12</sup> and Pt<sup>13</sup> additions to increase the 211 volume fraction while decreasing the particle size for flux pinning and mechanical enhancement. Other modifications include the powder melting process<sup>5</sup> and solid-liquid melt growth method,<sup>14</sup> which utilizes a mixture of  $\text{Y}_2\text{O}_3$ , CuO and  $\text{BaCuO}_2$  to replace the quenching step in MPMG, the melt quenched pressurized partial melt growth method,<sup>15</sup> which uses an external pressure to prevent liquid egression during melting, as well as MTG in the presence of a magnetic field<sup>16</sup> to align the 123 nuclei during the initial stage of solidification. Regardless of the method or modification, the common traits of nondirectional solidification are: (i) rapid heating to melting temperature with minimum dwell time to minimize the coarsening of 211 precipitates and (ii) slow cooling past the peritectic temperature to restrict the amount of nuclei and to develop the stacked plate microstructure.

Due to grain alignment,  $J_c$  of melt-processed 123 for current flowing along the  $a$ - $b$  planes within an oriented domain is quite high. Typical variation in  $J_c$  with applied magnetic field of an LPP specimen is shown in Fig. 1, in which it can be seen that the  $J_c$  remains at a relatively high value of  $10^4$  A/cm<sup>2</sup> in a field of several T. It can also be seen from the figure that the HTS is anisotropic, with a much weaker field dependency when the magnetic field is directed along the  $a$ - $b$  planes. This  $J_c$  anisotropy is shown in detail in Fig. 2, where two  $J_c$  peaks are seen; a narrow and intense peak is centered at  $H||a$ - $b$ , whereas a weaker and broader peak is located at  $H||c$ . While the  $J_c$  within an oriented domain is large, the value drops to the order of  $10^2$ – $10^3$  A/cm<sup>2</sup> when the transport current has to traverse the domain boundaries. Therefore, in

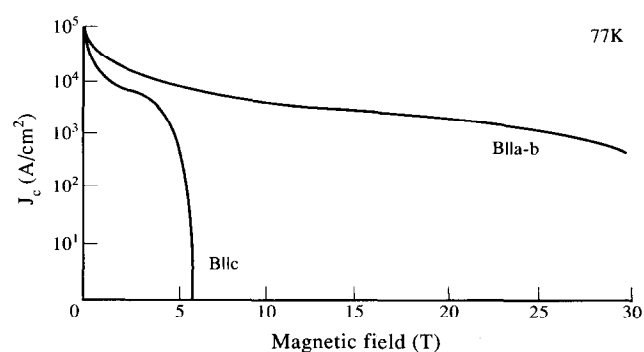


Fig. 1. Variation in  $J_c$  with  $B$  of LPP sample at 77 K.<sup>17</sup>

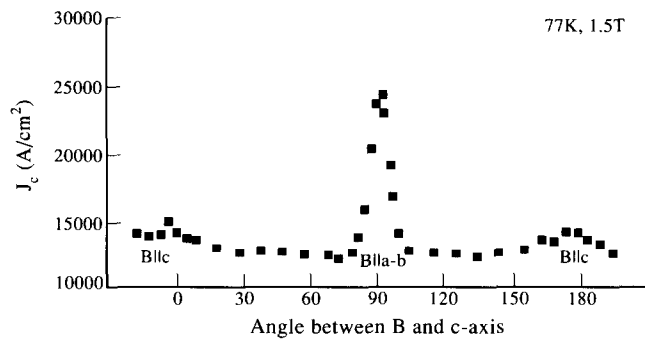


Fig. 2.  $J_c$  anisotropy of LPP sample at 77 K and 1.5 T.<sup>3</sup>

order to utilize these melt-textured HTS in practical applications, the size and alignment of these oriented domains have to be improved.

## 2.2 Directional solidification

In order to increase the dimensions of an oriented domain in melt-textured 123, both the grain nucleation and the growth direction have to be controlled. This can be accomplished by directional solidification. In the past few years, significant progress has been achieved in this area. Domain size, however, is not the only factor that limits the current capacity of the HTS. In addition, the strongly superconducting  $a$ - $b$  planes need to be aligned along the sample axis to obtain large critical currents ( $J_c$ ) as well as maintaining superconducting and mechanical stability of the HTS.

All directional solidification methods<sup>18–22</sup> involve the relative motion between the hot zone and the sample, which can be achieved by the movement of either the furnace or the sample. Also, a temperature gradient exists in the hot zone to provide the directionality in solidification. In the semi-continuous process developed by Meng *et al.*,<sup>18</sup> a multi-zone horizontal tube furnace with a prescribed temperature profile is utilized. A sintered 123 sample is transported through the furnace at a rate determined in conjunction with the temperature profile. By doing so, different parts of the sample are heated to 1100°C for a short time, rapidly cooled to 1050°C and then slowly cooled. Samples of 2.5×5×40 mm<sup>3</sup> have been produced by this method, and are found to possess a critical current of 400 A at 77 K.<sup>19</sup> In the zone melting process developed by McGinn *et al.*,<sup>20</sup> thin, extruded, presintered samples are directionally solidified in a vertical tube furnace with a hot zone temperature of 950–1050°C, and the solidification rate is controlled by the sample travelling rate. Because of the small cross-sectional area of the samples, the lateral temperature gradient does not appear to be significant, and grain alignment

along the sample axis has been achieved. When the sample cross-sectional area is increased, however, the  $a$ - $b$  planes of directionally solidified 123 are frequently aligned at an angle to the sample length. This is believed to be due to heat extraction from the sides of the sample, which results in a lateral temperature gradient. Therefore, in spite of an imposed longitudinal temperature gradient, the effective temperature gradient is directed at an angle to the sample axis such that inclined 123 grains nucleate and grow inward from the sides.<sup>23</sup>

To minimize the extent of heat extraction from the sides of the sample, Selvamanickam *et al.*<sup>22</sup> developed a modified Bridgman furnace, where an auxiliary heater is added to the process zone. The purpose of this heater is to raise the temperature at the periphery of the process zone, which results in a negative temperature gradient of 20°C/cm, i.e. the temperature at the sides of the sample is higher than that along the axis. The 60 mm hot zone of this furnace is maintained at 1050°C with a longitudinal temperature gradient of 50°C/cm at the process zone. Because of the magnitude of this temperature gradient, the travelling rate of the sample is chosen to be 1 mm/h, such that the temperature gradient to growth rate ratio ( $G/R$ ) is maintained above a critical value of  $\approx 350$ – $500^\circ\text{C}\cdot\text{h}/\text{cm}^2$ .<sup>24</sup> Because of the negative lateral gradient, 123 grains can be expected to nucleate from the interior of the sample. Samples 3×3 mm<sup>2</sup> in cross-section and up to 55 mm long have been grown using this method. Microstructural and X-ray pole figure analyses have shown that the grains are aligned parallel to the sample axis to within 10°. In addition, transport measurements along different sections of one sample revealed that a uniform  $J_c$  in excess of 20,000 A/cm<sup>2</sup> at self-field and 77 K can be obtained.

When the cross-sectional area of the sample is further increased, the lateral temperature gradient again becomes a problem, resulting in multiple misaligned domains. In addition to a lower  $J_c$ , the superconducting and mechanical stability of the sample is found to have worsened. This degradation is believed to be due to the anisotropic thermal expansion coefficient of the HTS. Since the domains are not free to contract during sample cooling, tensile stresses result in the  $c$ -direction of each domain. This coupled with the fact that the HTS is weakest along the  $c$ -axis lead to microcracking between the stacked plates. For these misaligned samples, the transport current has to flow past the plates and, therefore, the current carrying capability can be expected to decrease with the severity of microcracking. This degradation has indeed been found in samples subjected

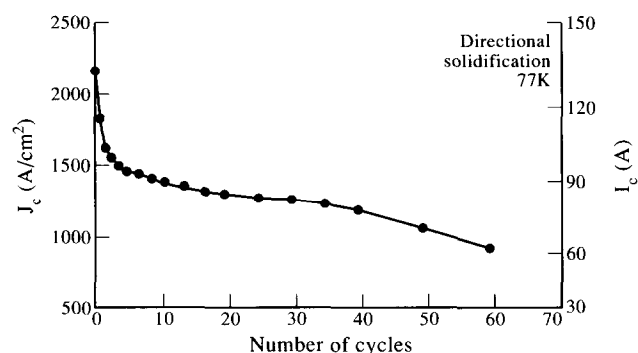


Fig. 3. Variation in current capacity with thermal cycling in directionally solidified 123.<sup>25</sup>

to thermal shocking between 373 and 77 K.<sup>25</sup> The variation in  $I_c$  with the number of thermal cycles in a misaligned directionally solidified 123 sample is shown in Fig. 3. It can be seen from this figure that  $I_c$  decreases with thermal cycling, with degradation of up to 50% in less than 10 thermal cycles. Microstructural analysis on the sample showed that both the amount and length of the microcracks have increased with thermal shocking. Since these microcracks are typically found between the 123 plates, an obvious way to minimize the effect of cracking on the  $I_c$  is to obtain textured 123 with a single domain and grain alignment along the sample axis.

### 2.3 Seeded growth

During the past year, seeding of 123 has emerged as a dominant texturing method to obtain large 123 domains with predetermined grain orientation. Single crystal and melt-textured Sm-123 (or Nd-123) have been shown to be effective seeds for the Y-123 HTS.<sup>13</sup> These seeds are found to operate as nucleation centres where the crystal orientation of the growth matches that of the nucleation source. Since the seed has a higher peritectic temperature than that of the Y-123, it remains in a solid form, while the Y-123 is in a semi-solid state. On subsequent cooling, epitaxial growth of Y-123 occurs at the Sm-123/Y-211 + Liquid interface, where the orientation of the solidifying Y-123 matches that of the seed, in order to minimize the strain energy. With seeding, the crystal orientation of the HTS can be customized to fit the geometry of the sample. An example of a successful seeding method is the top-seeded modified MTG, which is used to fabricate large-domained disks for magnetic levitation applications.<sup>26–29</sup> Before any seeding method can commence, suitable seeds need first to be obtained. One way to fabricate the Sm-123 seeds is by using the LPP method.<sup>7</sup> In this process, a bulk sintered Sm-123 is rapidly heated to 1130°C and

held at this temperature for 30–60 min to allow for complete decomposition. The sample is then rapidly cooled to 1065°C, where slow cooling commences at a rate of 0.5°C/h. It should be mentioned that the processing temperatures used in the LPP fabrication of Sm-123 are higher than the usual profile because the characteristic temperatures of Sm-123 are higher. After the temperature has reached 1000°C, the sample is cooled rapidly to room temperature to encourage cracking between the  $a$ – $b$  planes. The resulting melt-textured Sm-123 typically consists of oriented domains of 1.5 cm in size. To fabricate the seeds, single-domained Sm-123 are cut from the bulk, and the  $a$ – $b$  planes are exposed by cleaving along the cracks.

In the top-seeded modified MTG method, a Sm-123 seed is either placed or embedded on top of a Y-123 disk with its  $a$ – $b$  plane surface in contact with the disk. The sample together with the seed is then heated to 1030–1040°C and held for 1 h. After the holding period, the temperature is reduced at a rate of approximately 1°/h to 925°C, and then cooled to room temperature at a moderate rate. Cylindrical HTS with  $a$ – $b$  planes parallel to the top surface and up to 3–5 cm in diameter have been fabricated by this method.<sup>26–29</sup> The  $c$ -axis dimension, however, can vary due to grain impingement from nucleation sites at the bottom substrate interface. To minimize this problem and to increase the  $c$ -axis thickness, modifications such as the usage of a vertical chemical gradient have been developed.<sup>13</sup>

While top-seeded modified MTG can provide Y-123 disks with large oriented domains, the method is not suitable for fabricating HTS in conductor form. We have recently developed a seeded directional solidification method, which combines the ability to control the growth front with seeding.<sup>30</sup> In this method, a rectangular parallelepiped Sm-123 seed is cut and polished such that the edges are along the  $\langle 100 \rangle$  directions and the  $a$ – $b$  planes are parallel to the large surfaces. The seed is then embedded into a presintered Y-123 bar, and the sample is attached to a water-cooled holder. For directional solidification, the whole assembly is introduced into the hot zone of a modified Bridgman furnace for approximately 15–30 min, and then withdrawn at a rate of 0.8–1 mm/h. As the growth front of Y-123 passes by the Sm-123, seeded growth of Y-123 occurs at the interface. Samples of 4×8 mm<sup>2</sup> in cross-section and up to 55 mm long have been fabricated by this method. Optical and scanning electron microscopy revealed that the samples are single-domained with the  $a$ – $b$  planes in the domain being parallel to the sample axis. In addition, the maximum  $a$ - and  $b$ -axes

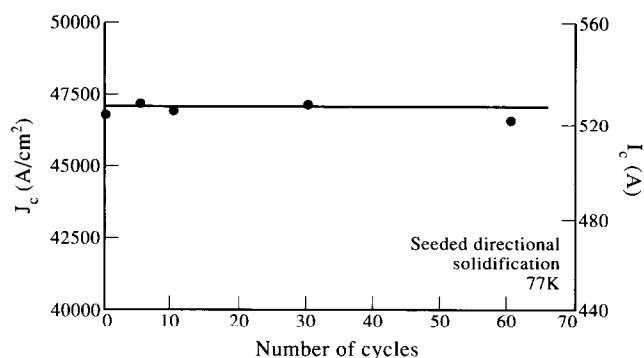


Fig. 4. Variation in current capacity with thermal cycling in seeded directionally solidified 123.<sup>25</sup>

deviation ( $c$ -twist) along the entire length is roughly  $5^\circ$ . Because of the favorable alignment of the strongly superconducting  $a$ - $b$  planes, the  $I_c$  of these samples is much higher than the 1,000 A capability available at this laboratory. Small cross-sectional area samples cut along the sample axis provided a  $J_c$  value of 46,000 A/cm<sup>2</sup> at 77 K and self-field, indicating that the  $I_c$  is at least several thousand amperes. In addition to the large current capacity, the superconducting stability of the HTS has also been improved by seeded directional solidification. As seen in Fig. 4, the current carrying capability of the sample is not affected by thermal shock of up to 60 cycles. This behaviour can be expected, since any microcracking between the 123 plate will be parallel to the current direction, and will not inhibit the current transport.

## 2.4 Recrystallization

One of the major problems associated with melt-texturing by solidification from the melt is the slow growth rate necessary to maintain growth front stability. Recently, a recrystallization method that has the potential to speed up the processing time has been developed.<sup>31</sup> These investigators found that when the 123 precursors are quenched from the  $Y_2O_3$  + Liquid state, 123 can recrystallize rapidly if the quenched material is subjected to suitable heat treatment above 500°C (123 formation time is less than 3 min at 890°C). Based on this finding, they developed a quench and directional recrystallization process that can form the textured microstructure without involving solidification from the melt. In this method, 123 powder is heated to 1400°C in a Pt boat at 700°C/h and held at this temperature for 2 h. After the powder has totally decomposed, the semi-solid melt is splat-quenched between two copper plates to room temperature. The quenched material is then ground and hot pressed at 400°C to form a bulk compact without being converted into the 123 phase. Direc-

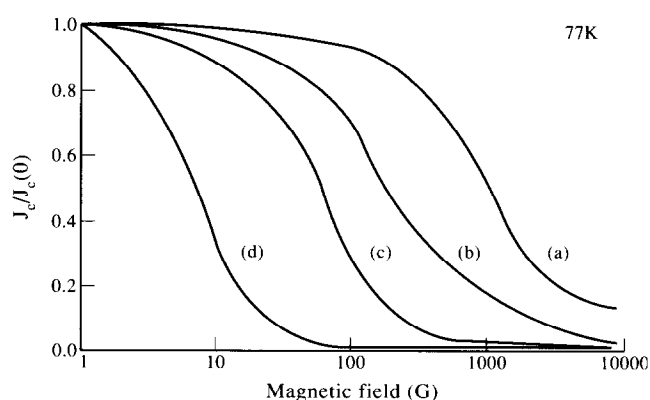


Fig. 5. Field dependency of normalized  $J_c$  at 77 K in 123 fabricated by (a) LPP, (b) quench and directional recrystallization, (c) magnetic alignment and (d) sintering.

tional recrystallization of the compact is performed in a travelling heater system where the peak temperature is maintained at 940°C, the sample entrance temperature gradient is 130°C/cm and the exit gradient is 225°C/cm. Because of the rapid recrystallization time of the quenched powder, a sample travelling rate of 10 mm/h is used.

Samples processed in such a fashion are found to consist of well-textured grains of 123 and CuO, aligned relatively parallel to each other (the CuO phase can be eliminated by Pt addition in the starting material). In addition, small 211 precipitates are found to be distributed throughout the sample. The textured area is seen to extend over 15 mm and is representative of the microstructure in the interior of the sample. Within the textured area, the spread in the 123 orientation is determined to be approximately  $15^\circ$ , indicating that there are several domains along the sample length. Although the sample consists of multiple domains, the relatively small deviation angle along the sample axis indicates that misorientation between neighbouring domains is small, and the domain boundaries are not the result of grain impingement. The zero field  $J_c$  of this sample is found to be 2,500 A/cm<sup>2</sup> at 77 K. Furthermore, the field dependency of  $J_c$  is superior to those of sintered and magnetically aligned 123 bulk HTS as seen in Fig. 5. Since the fabrication temperature of the process is low, the method may lend itself to rapid wire fabrication by combining with processes such as silver powder-in-tube.

## 3 SUMMARY

In the past few years, significant progress has been achieved in  $J_c$  enhancement of HTS by melt-texturing. Since the location of the solidification front as well as the growth direction can be

controlled through directional solidification, this method appears to be well-suited to the fabrication of long HTS in conductor form. Misalignment problems associated with the existence of a lateral temperature gradient in large cross-sectional area samples can now be controlled through seeded directional solidification. In addition to HTS in conductor form, seeding can also be used to produce disk-shaped HTS with large oriented domains for levitation applications. Instead of solidification from the melt, texturing can also be achieved through the recrystallization of quenched powder. This process has the potential of producing long wires, since the recrystallization temperature is lower than the melting temperature of several potential cladding materials.

## ACKNOWLEDGEMENTS

The authors would like to thank Dr V. Selvamanickam for his valuable discussion. They would also like to thank Messrs C. S. Partsinevelos and R. G. Presswood Jr for their assistance in this work.

## REFERENCES

1. SALAMA, K., RAVI-CHANDAR, K., SELVAMANICKAM, V., LEE, D. F., REDDY, P. K. & RELE, S. V., *J. Metals*, **40** (1988) 6.
2. JIN, S., TIEFEL, T. H., SHERWOOD, R. C., DAVIS, M. E., VAN DOVER, R. B., KAMMLOTT, G. W., FASTNACHT, R. A. & KEITH, H. D., *Appl. Phys. Lett.*, **52** (1988) 2074.
3. SALAMA, K., SELVAMANICKAM, V. & LEE, D. F., In *Processing and Properties of High- $T_c$  Superconductors: Vol. 1—Bulk Materials*, ed. S. Jin. World Scientific, Singapore, 1993, p. 155.
4. HOJAJI, H., BARKATT, A., HU, S., MICHAEL, K. A., THORPE, A. N., TALMY, I. G., HAUGHT, D. A. & ALTERESCU, S., *Mat. Res. Bull.*, **25** (1990) 765.
5. ZHOU, L., ZHANG, P., JI, P., WANG, K., WANG, J. & WU, X., *Supercond. Sci. Technol.*, **3** (1990) 490.
6. LEE, D. F., CHAUD, X. & SALAMA, K., *Jpn J. Appl. Phys.*, **31** (1992) 2411.
7. SALAMA, K., SELVAMANICKAM, V., GAO, L. & SUN, K., *Appl. Phys. Lett.*, **54** (1989) 2352.
8. CIMA, M. J., FLEMINGS, M. C., FIGUEREDO, A. M., NAKADE, M., ISHII, H., BRODY, H. D. & HAGGERTY, J. S., *J. Appl. Phys.*, **71** (1992) 1868.
9. IZUMI, T., NAKAMURA, Y. & SHIOHARA, Y., *J. Mater. Res.*, **7** (1992) 1621.
10. IZUMI, T., NAKAMURA, Y. & SHIOHARA, Y., *J. Mater. Res.*, **8** (1993) 1240.
11. MURAKAMI, M., GOTOH, S., FUJIMOTO, H., YAMAGUCHI, K., KOSHIZUKA, N. & TANAKA, S., *Supercond. Sci. Technol.*, **4** (1991) S49.
12. LEE, D. F., SELVAMANICKAM, V. & SALAMA, K., *Physica C*, **202** (1992) 83.
13. MORITA, M., TAKEBAYASHI, S., TANAKA, M., KIMURA, K., MIYAMOTO, K. & SAWANO, K., *Adv. Supercond.*, **4** (1991) 733.
14. VARANASI, C., SENGUPTA, S., MCGINN, P. J. & SHI, D., *J. Appl. Supercond.*, **2** (1994) 117.
15. HU, S., HOJAJI, H., BARKATT, A., BOROOMAND, M., HUNG, M. & BUECHELE, A. C., In *HTS Materials, Bulk Processing and Bulk Applications*, ed. C. M. Chu, W. K. Chu, P. H. Hor and K. Salama. World Scientific, Singapore, 1992.
16. LEES, M. R., BOURGAULT, D., BRAITHWAITE, D., DE RANGO, P., LEJAY, P., SULPICE, A. & TOURNIER, R., *Physica C*, **191** (1992) 414.
17. EKIN, J. W., SALAMA, K. & SELVAMANICKAM, V., *Nature*, **350** (1991) 26.
18. MENG, R. L., KINALIDIS, C., SUN, Y. Y., GAO, L., TAO, T. K., HOR, C. H. & CHU, C. M., *Nature*, **345** (1990) 326.
19. FRANCAVILLA, T. L., MENG, R. L., HOR, P., CHU, C. W., EKIN, J. W. & LIEBENBERG, D. H., *Cryogenics*, **33** (1993) 256.
20. MCGINN, P., CHEN, W., ZHU, N., LANAGAN, M. & BALACHANDRAN, U., *Appl. Phys. Lett.*, **57** (1990) 1455.
21. PARISH, M. V. & CHANDLER, D. B., In *HTS Materials, Bulk Processing and Bulk Applications*, ed. C. M. Chu, W. K. Chu, P. H. Hor and K. Salama. World Scientific, Singapore, 1992.
22. SELVAMANICKAM, V., PARTSINEVELOS, C. S., MCGUIRE, A. V. & SALAMA, K., *Appl. Phys. Lett.*, **60** (1992) 3313.
23. SALAMA, K. & LEE, D. F., *Supercond. Sci. Technol.*, **7** (1994) 177.
24. IZUMI, T., NAKAMURA, Y. & SHIOHARA, Y., *Adv. Supercond.*, **4** (1991) 429.
25. LEE, D. F., SATPATHY, A., SELVAMANICKAM, V. & SALAMA, K., *Supercond. Sci. Technol.*, **8** (1995) 423.
26. GAO, L., XUE, Y. Y., RAMIREZ, D., HUANG, Z. J., MENG, R. L. & CHU, C. M., *Appl. Phys. Lett.*, **63** (1993) 260.
27. WEINSTEIN, R., REN, Y., LIU, J., CHEN, I. G., SAWH, R., OBOT, V. & FOSTER, C., *Physica C*, **251** (1995) 15.
28. BLOHOWIAK, K. Y., GARRIGUS, D. F., LUHMAN, T. S., MCCRAY, K. E., STRASIK, M., AKWAY, I. A., DOGAN, F., HICKS, W. B., LIU, J. & SARIKAYA, M., *IEEE Trans. Appl. Supercond.*, **3** (1993) 1049.
29. HASHIMOTO, M., TANAKA, M., MORITA, M., KIMURA, K., TAKEBAYASHI, S., TESHIMA, H., SAWAMURA, M. & MIYAMOTO, K., In *Proc. 6th US-Japan Workshop on High  $T_c$  Superconductors*, ed. K. Salama, C. W. Chu & W. K. Chu. World Scientific, Singapore, 1994, p. 89.
30. LEE, D. F., PARTSINEVELOS, C. S., PRESSWOOD, Jr, R. G. & SALAMA, K., *J. Appl. Phys.*, **76** (1994) 603.
31. SELVAMANICKAM, V., GOYAL, A. & KROEGER, D. M., *Appl. Phys. Lett.*, **65** (1994) 639.